Contactless Thin-Layered Torque Sensor Module with Fully-digital Signal Processing Circuit

Chi-Ting Yeh[1], Nan-Chyuan Tsai[1], Hsin-Lin Chiu[1] and Chung-Yang Sue[2]

[1]*Department of Mechanical Engineering, National Cheng Kung University, 70101, Tainan City, Taiwan*
[2]*Industrial Technology Research Institute, 734, Tainan City, Taiwan*

Keywords: Torque Sensor, Orange-slice-alike Flexible Body, Fully-digital Signal Processing Circuit, Optical Grating.

Abstract: A contactless thin-layered torque sensor with fully-digital signal processing circuit is proposed in this work. The mechanical structure of the torque sensor is an orange-slice-alike flexible body. Two links, beforehand aligned, with B/W stripes play the role of optical grating by resolution 1° as no any torque applied to the shaft. As long as the orange-slice-alike flexible body, sandwiched by the aforesaid links, is subject to an external torque applied, a twisted angle is induced between the two thin photo-grating discs. Two sets of photo detector cooperate with the two discs with optical gratings to generate two pulse sequences. Therefore, a time delay between these two pulse sequences can be acquired as long as the shaft is twisted by a torque. A counter IC is employed to quantify this time delay in terms of the torque applied, and the time period, in terms of rotational speed of shaft. One of merits of the proposed torque sensor is: real-time measurement on torque applied becomes feasible even if the shaft, subject to external torque, is rotating at high speed. Another advantage of the fully-digital signal processing circuit is: no need to conduct A/D conversion and free of noise, cross-talk and EMI (Electromagnetic Interference).

1 INTRODUCTION

The operation principle of a torque sensor is to quantify the angular deformation of a shaft which is subject to an external torque if the torsional stiffness is known beforehand. Torque sensors are often applied to monitor the input/output torques for a wide variety of industries such as numerous types of motors, generators, engines, torque wrenches and etc. No doubt the role of torque sensor is pretty significant in control/servo systems as well.

The traditional torque sensors apply strain gauges to derive the torque exerted on the shaft. The induced voltage signals are exported by the embedded carbon brushes and the slip ring at the strain gauge unit. The type mentioned above is so called "contact-type". As well known, it has many shortcomings such as the undesired abrasion caused by the relative rotation between carbon brush and slip ring so that the lifespan of torque sensor is short and the measurement error is high. Therefore, non-contact type torque sensors are developed afterwards.

In addition, the shape of rotary torque transducer is usually and popularly designed to be of long cylinder due to consideration of easier mass production. However, after being installed with robot arms, the overall length of the resulted equivalent robot arm is much increased. This results in more control complication and more room required. Therefore, the tendency of new design is trying its best to reduce the axial thickness of cylindrical torque sensors. Nevertheless, the current commercial rotary torque sensors with thin thickness are mostly of contact-type. In other words, their performance is determined quite much by the corresponding electronic facilities, circuit and temperature correction technique. Besides, the output signals of rotary thin torque sensors are all analog. It leads to another serious concern: electric interference such as EMI, cross-talk and noise.

In recent years, various researches regarding torque sensors were proposed. An optical type of torque sensor applied for the arm of humanoid robot was designed by Tsetserukou et al. (Tsetserukou, 2006). Another optical torque sensor using compliant suspension to suppress measurement crosstalk is presented by Kaminaga et al. (Kaminaga, 2011). Though their torque sensor is of non-contact, the corresponding output signal is still analog. On the other hand, multi-axes torque sensors gradually

attract intensive attentions. A six-axes wrist force/moment sensor was proposed by Kim applied for an intelligent robot (Kim, 2007). Liang et al. presented another type of six-dimensional wrist force/torque for five-axes parallel machine tool (Liang, 2010). In addition to optical torque sensors, a six-axis capacitive-type force-torque sensor is designed and realized to measure the power transfer between the human body and the environment (Brookhuis, 2014). Besides, a capacitor-type torque sensor, capable to measure the full angular torque range, is proposed to apply upon magnetic anisotropies (Rigue, 2012). Unfortunately, the aforesaid torque sensors are not applicable to rotary shafts, particularly for high speed mode.

To count for the shortcomings of the torque sensors discussed above, a contactless thin-layered torque sensor with fully-digital signal processing circuit is hence proposed in this work. The proposed torque sensor possesses a lot of merits such as low cost, free maintenance, thin thickness, light weight, adaptive to be applied to high-speed rotors, and no signal interference at all. Compared with the traditional torque sensors, the advantages of the proposed sensor are listed in Table 1.

This proposed digital torque sensor can be employed for numerous applications such as machine tools, robot arms, spindles of power tools, washing machines and etc. Due to its merits of free contact and noise, its measurement precision can be retained all the time even under serious contamination environments.

Table 1: Comparison between traditional and proposed torque sensors.

Compared with analog torque sensors	Compared with rotary (brush embedded) torque sensor
Lower cost	Can operate in high speed
No signal interference	No brush wear
No need to compensate temperature correction	No noise out of carbon brush
Lower demand on the performance requirements of associated photo reflectors	Longer lifespan and more reliability

2 DESIGN OF CONTACTLESS THIN-LAYERED TORQUE SENSOR

To design a torque sensor applied to robot arms with high-speed shafts, it is expected to meet a few goals: (i) thin along axial direction, (ii) able to operate under high-speed rotation mode, (iii) able to real-time measure the torque exerted on the shaft, with no considerable time delay.

2.1 Thin and Flexible Mechanical Structure

The profile and the parameters of proposed thin orange-slice-alike flexible body are shown in Figure 1. The basic design concept of the mechanical structure is to take advantage of elastic deformation of the metal texture to reflect the exerted torque. One outer ring and six palm anchors are combined to construct the main part of the orange-slice-alike flexible body. To enhance more sensitivity to the exerted torque, the outer ring and the palm anchors are radially connected by spokes so that the cross-section of the mechanical structure therefore looks like an orange slice. The parameters and dimensions of the spokes can be obtained by consideration of the overall volume of the torque sensor as small as possible but its precision and resolution as high as possible. Aside, a few screw holes are made on the outer ring and palm anchors for connecting the associated linkers and the orange-slice-alike flexible body. If an external torque was applied to this mechanical structure, the twelve spokes would be twisted at the same time such that the deformations of twelve spokes would together result in a relative angular displacement between the outer ring and palm anchors. Based on the assumption that the torsional stiffness of the orange-slice-alike flexible body is constant, the applied torque can be quantified *via* the evaluation of this induced twisted angle. Compared with the design of non-coplanar flexible structure (Renaud, 2009), the sensitivity and reliability of proposed orange-slice-alike flexible body by authors is evidently much superior.

How to design the profile of the orange-slice-alike flexible body directly affects the performance of the resulted torque sensor, including the achievable range of measurement, the rotational speed span compatible with the torque sensor equipped (operation bandwidth), resolution, linearity and so on. Hence, firstly the mechanical design is focused on: the orange-slice-alike flexible body can
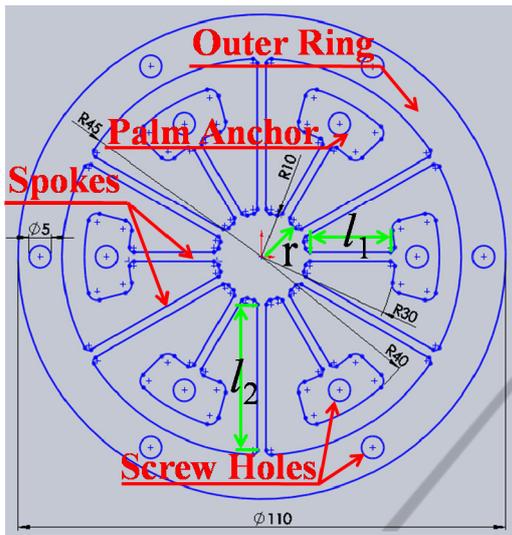
Figure 1: Profile of Thin Orange-slice-alike Flexible Body (Dimensions in mm).

result in a twisted angle as large as possible but still it has to be fully secure by ensurance of sufficient fatigue strength. By assuming spokes of the orange-slice-alike flexible body are cantilever beams, the relation between the bending moment and the resulted maximum normal stress at the free end of the cantilever spoke is as follows:

$$\sigma_{max} = \frac{Mc}{I} = \frac{6M}{Nbt^2} < fatigue\ strength \qquad (1)$$

where N, b, and t are the numbers, width, thickness of the spokes respectively. M is maximum torque applied to the orange-slice-alike flexible body. I is the moment of inertia of rectangular cross-sectional area of the spoke.

$$I = \frac{bt^3}{12} \qquad (2)$$

The fatigue strength depends on the material chosen. Once the material of orange-slice-alike flexible body is chosen, Nbt^2 can be considered as a constant, α.

$$Nbt^2 = \alpha = const. \qquad (3)$$

On the other hand, the spring constant of the orange-slice-alike flexible body can be derived as follows (Shams, 2012):

$$k_s = 4NEI(\frac{1}{l_1} + \frac{3r}{l_1^2} + \frac{3r^2}{l_1^3})(\frac{1}{l_2} + \frac{3r}{l_2^2} + \frac{3r^2}{l_2^3})/$$
$$(\frac{1}{l_1} + \frac{3r}{l_1^2} + \frac{3r^2}{l_1^3} + \frac{1}{l_2} + \frac{3r}{l_2^2} + \frac{3r^2}{l_2^3}) \qquad (4)$$

where l_1 and l_2 are the spoke lengths for connecting the palm anchor and the outer ring to the geometric

center of mechanical structure respectively, E modulus of elasticity of material, and r inner radius of the orange-slice-alike flexible body. By replacing length-related terms by equivalent length, L_e, the spring constant can be simplified as follows:

$$k_s = 4NE\frac{bt^3}{12}L_e^{-1} = E\frac{\alpha t}{3}L_e^{-1} = \frac{M}{\theta} \qquad (5)$$

The product of the twisted angle and thickness of spokes can be obtained:

$$\theta \cdot t = \frac{3M}{E\alpha L_e^{-1}} = Const. \qquad (6)$$

The larger θ in Eq. (6), the smaller t has to be. Once t is settled, the length of spokes can be determined simultaneously.

2.2 Computer Simulations of Orange-slice-alike Flexible Body Subject to Torque

Aluminium Alloy 7075-T6 is chosen as the material of the orange-slice-alike flexible body. The fatigue strength of 7075-T6 is 159MPa (Was, 1981). The relation between the twisted angle of orange-slice-alike flexible body and the applied torque is developed by the commercial software *ANSYS* and shown in Figure 2. The case in Figure 2 is a 4 N-m torque applied on the orange-slice-alike flexible body under rotational speed being 20000 RPM. The maximum stress, shown in Figure 2, is about 90MPa. It is far below the fatigue strength of 7075-T6 (about 57%). Besides, the resulted twisted angle with respect to the applied torque 4 N-m is shown in Figure 3. It is evident to find the property of high linearity in terms of twisted angle to torque. The resulted twisted angle of the torque sensor is 1.042° as a torque 4 N-m is applied. Finally, the photograph of the corresponding torque sensor successfully manufactured is shown in Figure 4.

2.3 Optical Grating and Light Receiver

To realize the proposed torque sensor applied to high-speed shafts, a couple of reflective photo detectors and the associated reflectors with black/white strips, shown in Figure 5, are equipped. As the light by light-emitting element shoots onto the white strips on reflector, shown in Figure 5(a), the light will be reflected to the photo receiver and hence an output voltage is generated by the photo detector. On the contrary, no output signal is generated if the light by light-emitting element
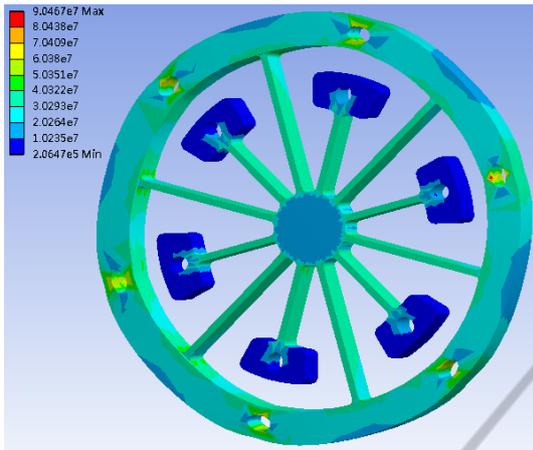
Figure 2: Stress Distribution on Orange-slice-alike flexible body by Torque: 4 N-m and Speed: 20000 RPM (Unit of Stress: Pa).
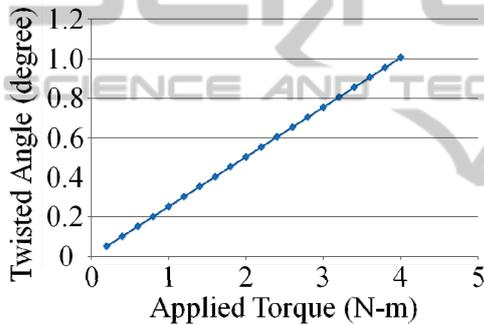

Figure 3: Relation between Twisted Angle and Applied Torque.

Figure 4: Photograph of Orange-slice-alike flexible body.

shoots onto the black strips, shown in Figure 5(b). The pulse-type output signal is therefore generated in sequence by the photo detectors all the time as the shaft is either still or rotating at high speed. For simplicity, the upper module and lower module shown in Figure 5 will be hereafter called as "photo detector" and "photo reflector" respectively.

Figure 5: Schematic Diagram of Reflective Photo Detector.

As the shaft is rotating, the orange-slice-alike flexible body and two photo reflector units are rotating as well because they are all fixed and attached to the shaft. Instead, the reflective photo detectors are not rotating at all because they are apart and completely separated away from the shaft. By any one of the photo detectors, the rotational speed of the shaft can be obtained since it plays the role of encoder as well. It is noted that beforehand these two photo reflectors have to be completely aligned under the circumstance: no any torque applied. Figure 6(a) is referred to this case: no torque applied. Most importantly, the trigger signals to these two photo detectors, to generate the pulse sequences, have to be synchronized all the time. Once the orange-slice-alike flexible body is deformed by external torque, the two reflectors will be also twisted and an angle, i.e., the relative angular displacement, is induced. Figure 6(b) is referred to the case of an external torque applied. Therefore, the output signals out of the two corresponding reflective photo detectors will present a time difference or called time delay. This time delay can be utilized to quantify the torque applied to the shaft. The photograph of the entire contactless thin-layered torque sensor unit mounted to the shaft is shown in Figure 7.

3 FULLY-DIGITAL SIGNAL-PROCESSING CIRCUIT

The associated circuit to comply with the photo detectors is nothing but a type of fully-digital counter so that almost no signal interference is involved. The principle of counting is shown in Figure 8. The counter IC is reset and immediately starts to count after receiving the trigger signal at PIN 11 from *Reflective Photo Detector #1*. As the D-flip-flops receives the trigger signal at PIN 9 from *Reflective Photo Detector #2*, a number of counts

will be exported to the display. It is noted that two key parameters, T and T_1, are named as "time period" and "time delay" respectively. By physical meanings, T is determined by the rotational speed of shaft while T_1 by how much the torque is applied onto the shaft. That is, the larger torque, the larger T_1.
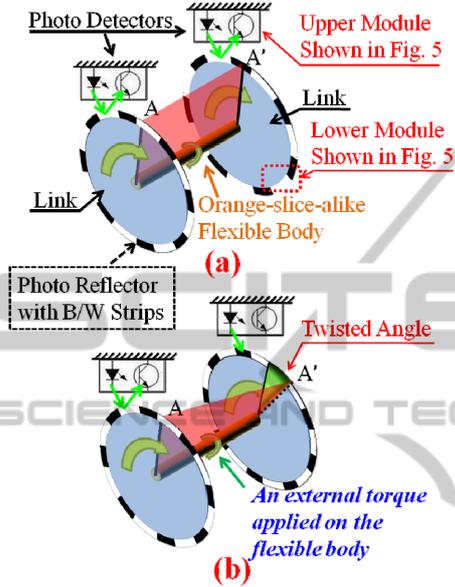

Figure 6: Schematic Diagram of Photo Detectors and Photo Reflectors (a): no torque applied; (b): an external torque applied.
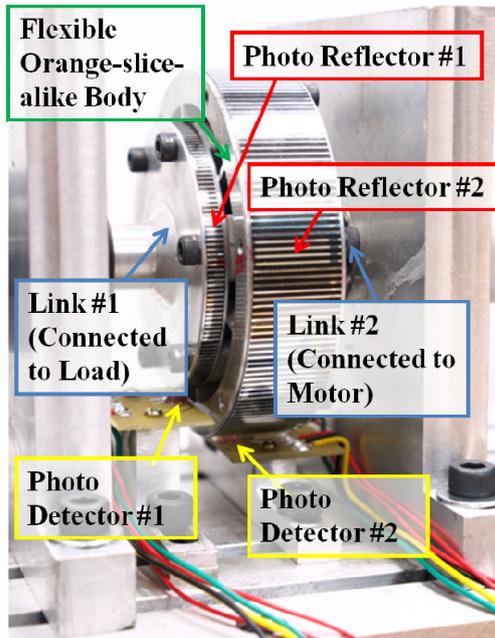

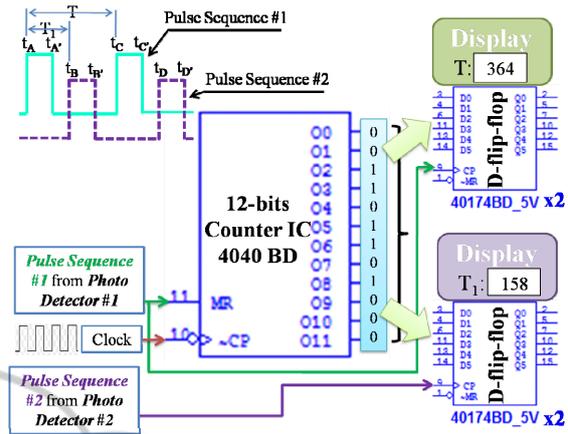Figure 7: Photograph of Contactless Thin Torque Sensor.

Figure 8: Schematic Diagram of Counter and Triggers.

The potential flaws by the signal-processing circuit without flip-flops are:

(a) : Missed count due to overlap of two pulse sequences.

(b) : The count numbers are running too fast to be instantly picked up.

How to overcome these two flaws is described in following sections.

3.1 Flaw #1: Missed Count Due to Overlap of Two Pulse Sequences

The duty cycle of either pulse sequence is determined by the rotation speed of shaft and the width of B/W strip on the photo reflector. Normally, the two pulse sequences, **Pulse sequence #1** and **Pulse Sequence #2**, are completely decoupled and shown in Figure 9(a). However, once the rotation speed of shaft is low and the width of B/W strip is relatively larger, the phenomenon of overlapped sequences occurs and is shown in Figure 9(b). The counter IC is triggered to start to count by PIN 11 which is defined as "high active". That is, during the time interval, $t_A \sim t_{A'}$, the counter IC is under the operation of triggering until $t_{A'}$. Unfortunately, if the applied torque is relatively smaller, **Pulse Sequence #2** is coming in just during this time interval, $t_A \sim t_{A'}$. This results in ignorance of the event which occurs at **Instant** t_B by counter IC so that the expected count for T_1 (i.e., from t_A to t_B) is missed at all. To solve this overlap problem, an inductor (L_R) is inserted and shown in Figure 10, in parallel to **Pulse Sequence #1**. The reason is stated as follows. Since an inductor is like a very-low-pass filter, at the instant t_A (i.e., sudden change from low

to high), the inductor is near "open" (i.e., cross-voltage to be high) but approaches to be near "close" (i.e., cross-voltage to be zero) as time goes away from instant t_A due to **Pulse Sequence #1** being kept to be flat from t_A to t_B. The cross-voltage of the inductor is shown in Figure 9(c) and 9(d), compared with the original **Pulse Sequence #1** in Figure 9(a) and 9(b), to which no any inductor inserted. That is, the impact of overlap between **Pulse Sequence #1** and **Pulse Sequence #2** is greatly reduced.
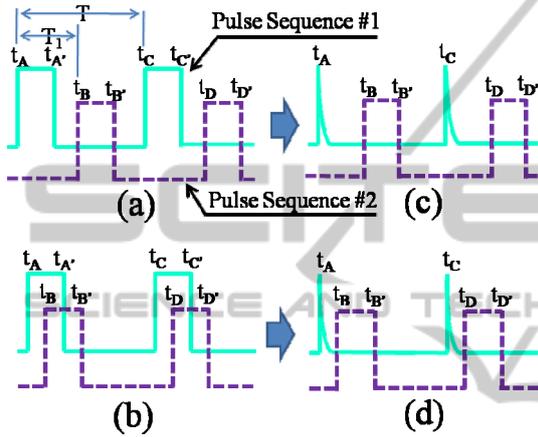

Figure 9: Effect by Additional Inductor Inserted to Counter Circuit (a) w/o Overlap and w/o Inductor Inserted; (b) with Overlap but w/o Inductor Inserted; (c) w/o Overlap but with Inductor Inserted; (d) with Overlap and with Inductor Inserted.
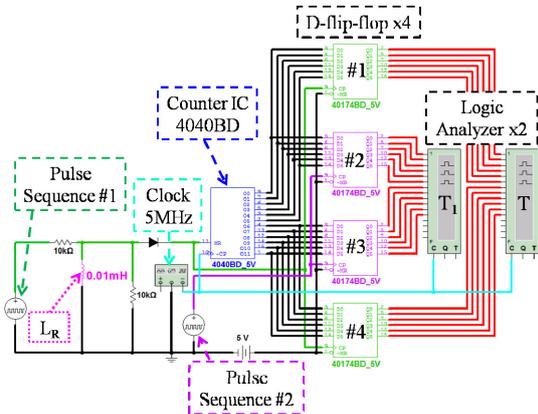

Figure 10: DSP Circuit for Computer Simulations.

3.2 Flaw #2: the Count Numbers Are Running Too Fast to Be Instantly Picked up

Since the data at count register is running very fast as long as the counter IC has been triggered, how to

real-time pick up the current-time count number to reflect the current-time torque applied has to be figured out. To solve this problem due to extremely dynamical data change of torque measurements, 4 units of D-flip-flop, shown in Figure 10, are added to the counter DSP circuit. Two of them (i.e., #1 and #4) are for T while the other two (i.e., #2 and #3) for T_1. The two flip-flops are employed to comply with the 12-digital counter IC since each D-flip-flop IC 40174BD is of 6-digit. That is, the D-flip-flop is operating like a buffer and temporary storage of the current-time count number.

3.3 Computer Simulations of Fully-digital Signal Processing Circuit

Assume the torque sensor has the property of linear stiffness for the orange-slice-alike flexible body. It would be twisted by one degree (i.e., 1°) if a torque 4 N-m was applied to the shaft. The computer simulation results for the DSP circuit as the shaft is rotating at 10000 RPM are shown in Figure 11. The count number, with respect to T_1, is 82 as a torque 4 N-m is applied to the shaft. In comparison, if the torque is reduced by 50%, i.e., 2 N-m, the corresponding count number is reduced to 40. It is observed that, the error of count is about 5% at high-speed rotation. On the other hand, if the rotation speed of shaft is reduced to 2000 RPM, the corresponding simulation results are shown in Figure 12. In Figure 12(a), the count number, with respect to T_1, is 384 as a 4 N-m external torque applied to the shaft. The count number is reduced to 192, shown in Figure 12(b), as the applied torque is reduced by 50%. There is no measurement error under low speed rotation. It is concluded that in order to improve the resolution and accuracy at high rotational speed, the physical quantity of the inductor connected in parallel to **Pulse Sequence #1**, L_R, has to be chosen properly or the associated circuit has to be equipped with a counter IC facilitated with a higher-frequency clock.

4 EXPERIMENTAL RESULTS

The experimental setup of the contactless thin-layered torque sensor is shown in Figure 13. A set of gap sensor, Model LK-031 by *Keyence Instrumentation Corporation*, is employed to acquire the angular displacements (i.e., twisted angles) of
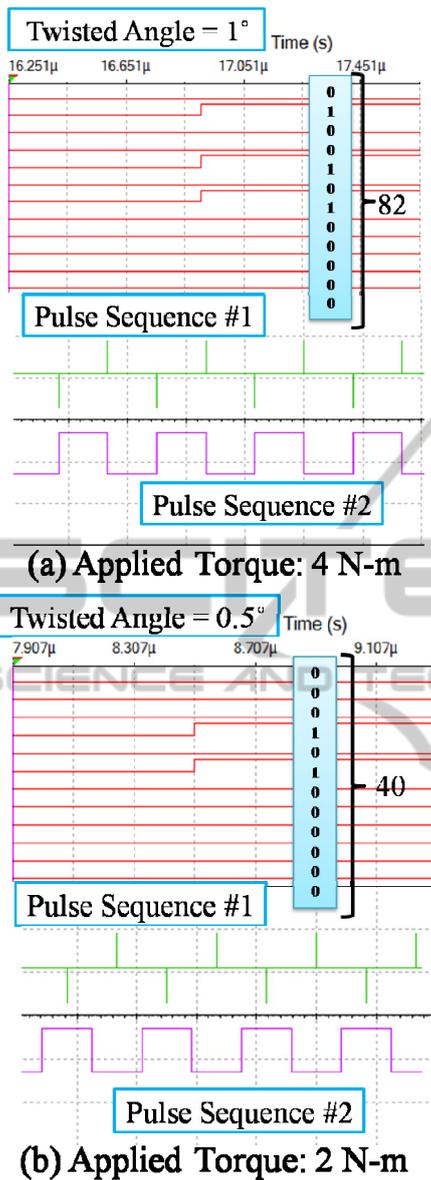
Figure 11: Count Numbers Versus Twisted Angles as Shaft is Rotating at 10000 RPM.

Figure 12: Count Numbers Versus Twisted Angles as Shaft is Rotating at 2000 RPM.

the orange-slice-alike flexible body for calibration propose, a high-precision torque sensor, Model 4520A by *Kistler Instrument Corporation*, is employed to acquire the applied torque to be compared with the proposed contactless thin-layered torque sensor. Besides, one compressed air brake, Model AHB-6 by *Magtrol Instrumentation Corporation*, is applied to reduced the speed of the shaft and protect the proposed torque sensor. The experiments are undertaken under the interface module cDAQ-8178 by *NI* and the environment by *Labview*. The contactless thin-layered torque sensor
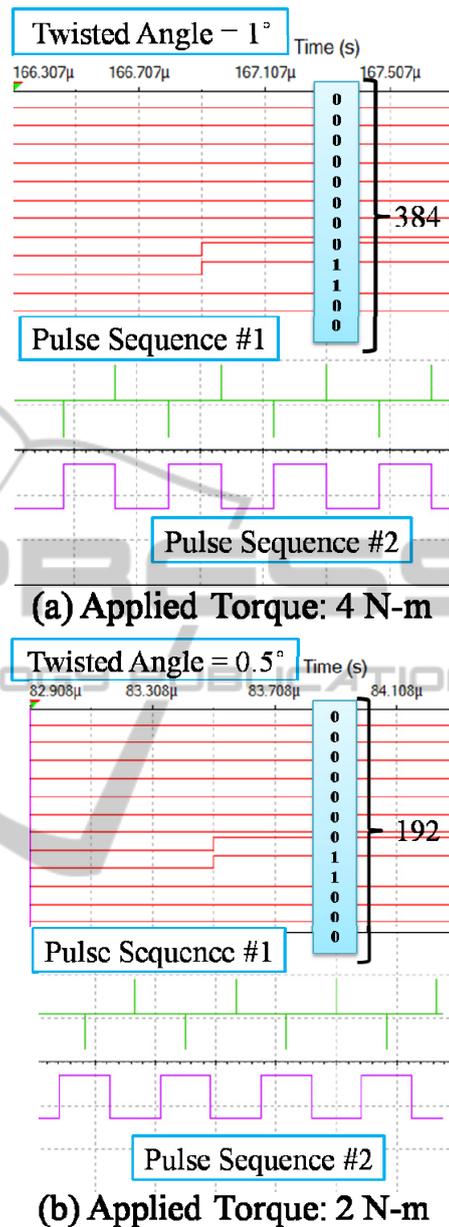
is examined for its hysteresis characteristics by applying torque in ascending/descending manner. The angular displacement and the applied torque are recorded by *Labview* to the storage of computer.

The graphic program by *Labview* to record the applied torque on the shaft and corresponding twisted angle is shown in Figure 14. The linear displacement, d_D, obtained by laser displacement sensor has already been converted into the twisted angle, θ_t, of the orange-slice-alike flexible body by
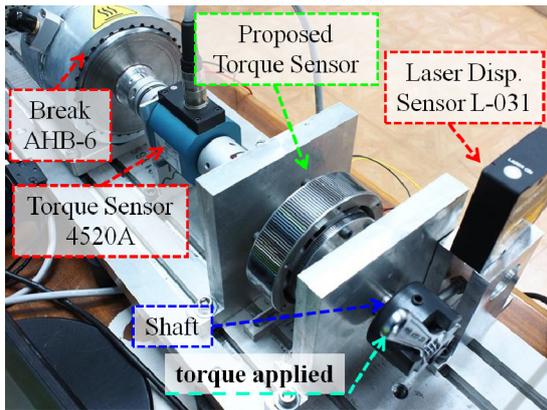
Figure 13: Experimental Setup for Proposed Torque Sensor.

the following rotation between d_D and θ_t :

$$\theta_t = \frac{d_D * 360}{2 * \pi * r_P} \qquad (7)$$

where θ_t is twisted angle of the orange-slice-alike flexible body. d_D is the linear displacement measured by the laser displacement sensor. $r_P = 58.4\,mm$ is the distance between the shaft and the laser displacement sensor. The real-time simulations of applied torque and twisted angle are shown at the bottom of Figure 14.
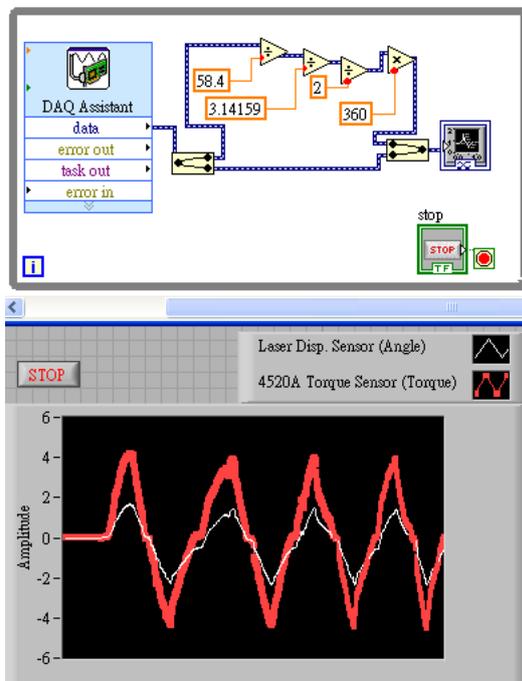

Figure 14: Graphic Simulation Program by *Labview* to Record Torque and Twisted Angle.

The hysteresis loop is shown in Figure 15. It is observed that the proposed torque sensor is with high linearity verified by the intensive experiments undertaken. However, the twisted angles by experiments are a little larger than those by computer simulations described in Section 2.2. This might be caused by the undesired deformation of the linker. At last, the repeatability of the proposed torque sensor in terms of applied torque to resulted counts by the DSP circuit, denoted by ***Loop 1***, ***Loop2*** and ***Loop 3***, is pretty superior.
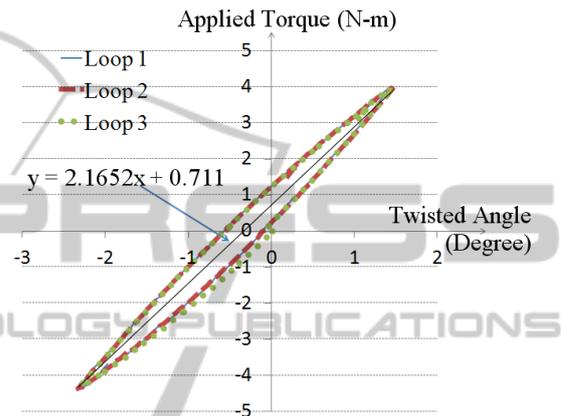

Figure 15: Hysteresis Loop of Proposed Torque Sensor.

5 CONCLUSIONS

A contactless thin-layered torque sensor with fully-digital signal processing circuit is proposed. The measurement range is up to torque 4 N-m and the rotational speed of shaft, compatible to the proposed torque sensor, up to 20000 RPM. The overall axial thickness of the torque sensor unit is only 42.6 mm. Compared with traditional torque sensors, the advantages of the proposed torque sensor are: (i) no need of analog/digital conversion for torque measurement, (ii) free of noise interference, (iii) due to its thin axial thickness, it is highly applicable for robot arms or multi-axes machine tools, (iv) it is also applicable for high speed shafts, and (v) it has the properties of high linearity in terms of applied torque with respect to twisted angle of the orange slice-alike flexible body, and superior repeatability in terms of torque measurement.

ACKNOWLEDGEMENTS

authors would like to express their appreciation.

REFERENCES

Tsetserukou, D., Tadakuma, R., Kajimoto, H., Tachi, S., 2006. Optical torque sensors for implementation of local impedance control of the arm of humanoid robot, *2006 IEEE Int. Conf. on Rob. and Auto.*, pp. 1674–1679.

Kaminaga, H., Odanaka, K., Kawakami, T., Nakamura, T., 2011. Measurement Crosstalk Elimination of Torque Encoder Using Selectively Compliant Suspension, *2011 IEEE Int. Conf. on Rob. and Auto.*, 2011.

Kim, G.-S., 2007. Design of a six-axis wrist force/moment sensor using FEM and its fabrication for an intelligent robot, *Sensors and Actuators A: Physical* 133(1), pp. 27–34.

Liang, Q., Zhang, D., Song Q., Ge, Y., Cao, H., 2010. Design and fabrication of a sixdimensional wrist force/torque sensor based on E-type membranes compared to cross beams, *Measurement* 43, pp. 1702–1719.

Brookhuis, R.A., Droogendijk, H., De Boer, M.J., Sanders, R.G.P., Lammerink, T.S.J., Wiegerink, R.J., Krijnen, G.J.M., 2014. Six-axis force–torque sensor with a large range for biomechanical applications, *Journal of Micromechanics and Microengineering* 24(3), Paper No. 035015.

Rigue, J., Chrischon, D., De Andrade, A. M. H., Carara, M, 2012. A torque magnetometer for thin films applications, Journal of Magnetism and Magnetic Materials, 324(8), pp. 1561-1564.

Renaud, P., Michel, M., 2009. Kinematic analysis for a novel design of MRI-compatible torque sensor, *2009 IEEE/RSJ Int. Conf. on Int. Rob. and Sys.*, pp. 2640-2646.

Shams, S., Lee, J.-Y., Han, C., 2012. Compact and lightweight optical torque sensor for robots with increased range, *Sensors and Actuators A: Physical*, 173, pp. 81-89.

Was, G. S., Pelloux R. M., Frabolot, M. C., 1981. Effect of shot peening methods on the fatigue behavior of alloy 7075-T6, *1th Int. Conf. on Shot Peening*, pp. 445-452.